ACS Infectious Diseases

Article

pubs.acs.org/journal/aidcbc

Chlorflavonin Targets Acetohydroxyacid Synthase Catalytic Subunit IlvB1 for Synergistic Killing of *Mycobacterium tuberculosis*

Nidja Rehberg,[†,¶] Herve Sergi Akone,[†,∥,¶] Thomas R. Ioerger,[‡] German Erlenkamp,[§] Georgios Daletos,[†] Holger Gohlke,[§] Peter Proksch,[*,†] and Rainer Kalscheuer[*,†]

[†]Institute of Pharmaceutical Biology and Biotechnology, Heinrich Heine University Düsseldorf, Universitätsstraße 1, 40225 Düsseldorf, Germany

[∥]Faculty of Science, Department of Chemistry, University of Douala, PO Box 24157, 2701 Douala, Cameroon

[‡]Department of Computer Science, Texas A&M University, 710 Ross St., College Station, Texas 77843, United States

[§]Institute of Pharmaceutical and Medicinal Chemistry, Heinrich Heine University Düsseldorf, Universitätsstraße 1, 40225 Düsseldorf, Germany

Supporting Information

ABSTRACT: The flavonoid natural compound chlorflavonin was isolated from the endophytic fungus *Mucor irregularis*, which was obtained from the Cameroonian medicinal plant *Moringa stenopetala*. Chlorflavonin exhibited strong growth inhibitory activity *in vitro* against *Mycobacterium tuberculosis* (MIC_{90} 1.56 μM) while exhibiting no cytotoxicity toward the human cell lines MRC-5 and THP-1 up to concentrations of 100 μM. Mapping of resistance-mediating mutations employing whole-genome sequencing, chemical supplementation assays, and molecular docking studies as well as enzymatic characterization revealed that chlorflavonin specifically inhibits the acetohydroxyacid synthase catalytic subunit IlvB1, causing combined auxotrophies to branched-chain amino acids and to pantothenic acid. While exhibiting a bacteriostatic effect in monotreatment, chlorflavonin displayed synergistic effects with the first-line antibiotic isoniazid and particularly with delamanid, leading to a complete sterilization in liquid culture in combination treatment. Using a fluorescent reporter strain, intracellular activity of chlorflavonin against *Mycobacterium tuberculosis* inside infected macrophages was demonstrated and was superior to streptomycin treatment.

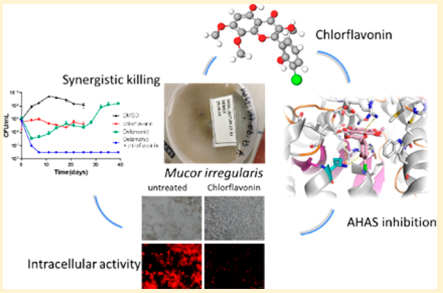

KEYWORDS: *chlorflavonin, Mycobacterium tuberculosis, acetohydroxyacid synthase, auxotrophy, synergistic killing effect*

Despite the availability of chemotherapy, a prophylactic vaccine, and a century of research, tuberculosis (TB), caused by the bacterium *Mycobacterium tuberculosis*, has resisted eradication and today is still a reason for major concern of health organizations and governments alike. Drug resistance is a major force causing the exacerbation of the TB pandemic, a problem which has steadily worsened during the past 20 years.[1] Multidrug-resistant *M. tuberculosis* strains (MDR-TB), which are resistant to the first-line antibiotics isoniazid and rifampicin, have developed into extensively drug resistant (XDR-TB) strains that are additionally resistant to any fluoroquinolone and one of the three injectable drugs capreomycin, kanamycin, and amikacin.[2] Some of these strains are resistant to all available antitubercular drugs and are virtually untreatable. The development of new anti-TB chemotherapeutics has been largely neglected by industrialized countries for decades as their development was deemed to be economically untenable. In recent years, however, there has been renewed interest in anti-TB drug development in the academic sector and lately also by the pharmaceutical industry. As a result of these efforts, several new antitubercular drugs are currently being evaluated in different stages of clinical trials.[3−5] Very recently, with the compounds bedaquiline and delamanid, the US Food and Drug Administration (FDA) and European Medicines Agency (EMA) have approved two new anti-TB drugs, with bedaquline representing the first clinical anti-TB drug of a novel class in 40 years.[6−8] However, due to potential side effects, these drugs were only approved for treatment of MDR-TB patients so far. Despite this success, it is clear that, with regard to effective control of the MDR- and XDR-TB pandemic in the future, the current efforts are by far not sufficient. Thus, new drugs for selective chemotherapy are still urgently needed for the fight against drug-resistant TB.

Like for the treatment of other bacterial infections, where compounds derived from nature account for ca. 70% of all currently available antibiotics,[9] natural products or their derivatives play crucial roles in modern day treatment of TB. Rifampicin is among the front-line therapeutic regime whereas other drugs derived from nature such as capreomycin, streptomycin, or cycloserine are in the second-line of treatment.[10] Thus, nature and its multitude of ingeniously

Received: April 21, 2017
Published: November 6, 2017

DOI: 10.1021/acsinfecdis.7b00055
ACS Infect. Dis. 2018, 4, 123−134

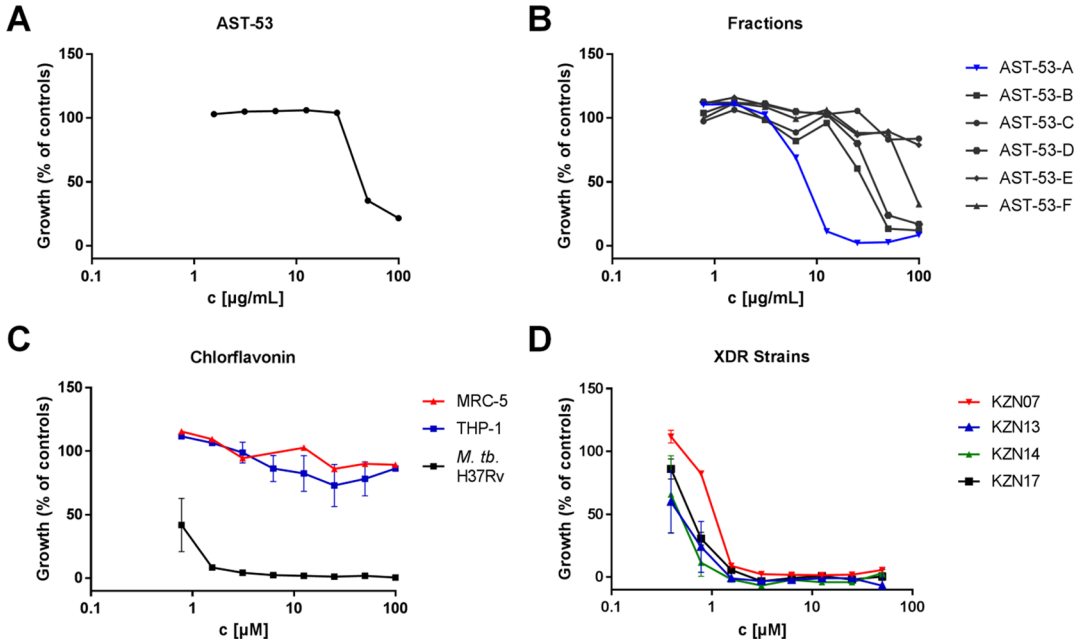

Figure 1. Potent and highly selective antitubercular activity of chlorflavonin. Dose–response curves of extract AST-53 (A) and of fractions AST-53 A-F (B) against *M. tuberculosis* H37Rv. (C) Dose–response curves of chlorflavonin against *M. tuberculosis* (*M. tb.*, H37Rv; black ■) and the human cell lines MRC-5 (red ▲) and THP-1 (blue ■). (D) Dose–response curves of chlorflavonin against *M. tuberculosis* XDR strains (KZN07, KZN13, KZN14, and KZN17). Data in (A) and (B) represent single measurements. Data in (C) and (D) are means of triplicates ± SD. Growth was quantified using the resazurin dye reduction assay.

synthesized natural products are a treasure chest in the quest for new anti-TB drugs.[11,12] However, the rate of discovery of new antibiotics from traditional terrestrial sources is decreasing. Thus, it is crucial to pursue less investigated organisms from unexplored habitats for bioprospection in the quest for novel anti-infectives. Fungal endophytes that live within the tissues of plants might represent a promising new source of novel anti-TB compounds as they are particularly rich in bioactive molecules as indicated by the steady rise of publications devoted to bioactive compounds from this group of organisms.

With this rationale, we investigated the anti-TB properties of extracts obtained from several endophytic fungi and identified the structurally unusual flavonoid chlorflavonin in a bioactivity-guided approach from the zygomycete *Mucor irregularis*, an endophytic fungus isolated from leaves of the Cameroonian medicinal plant *Moringa stenopetala*.

RESULTS AND DISCUSSION

Isolation and Antitubercular Activity of Chlorflavonin.

In continuation of our quest to identify novel molecules from nature with chemotherapeutic potential for the treatment of tuberculosis,[13] extracts from several endophytic fungi were tested for antibacterial activity against *M. tuberculosis* strain H37Rv employing the resazurin dye reduction method. The crude ethyl acetate extract AST-53 obtained from the endophytic zygomycetes *Mucor irregularis*, which had been isolated from fresh healthy leaves of the medicinal plant *Moringa stenopetala* collected in Cameroon and cultured on solid rice medium, showed inhibition against *M. tuberculosis* H37Rv with an MIC_{50} of 50 μg/mL (Figure 1A). This extract was taken to dryness and partitioned between *n*-hexane and 90% methanol. The 90% methanol fraction was subjected to vacuum liquid chromatography (VLC) on silica gel employing a step gradient of hexane–ethyl acetate and dichloromethane–methanol yielding 6 fractions (AST-53-A to AST-53-F) of which fraction AST-53-A exhibited the most pronounced enrichment in antitubercular activity with an MIC of 12.5 μg/mL (Figure 1B). Chromatography of fraction AST-53-A over Sephadex LH-20 and final purification by semipreparative HPLC yielded three known compounds identified as terphenyllin (**1**),[14] dechlorflavonin (**2**),[15] and chlorflavonin (**3**)[16,17] (Figure 2) by comparison of their NMR and mass spectroscopic data with literature (Table S1 and Figures S1–S6 for **3**). When testing these three compounds individually against *M. tuberculosis* cells, only chlorflavonin possessed antitubercular activity (Figures 1C and S7). A dose-dependent inhibition of growth was observed with an MIC_{90} of 1.56 μM. Remarkably, dechlorflavonin was completely inactive, indicating that the chlorine atom is crucial for the antibacterial property of chlorflavonin (Figure S7). In order to assess the cytotoxic potential of chlorflavonin against human cells, *in vitro* cytotoxicity studies were performed. Chlorflavonin showed virtually no cytotoxic effect against the two human cell lines THP-1 and MRC-5 up to the highest tested concentration of 100 μM, revealing a favorable selectivity index (IC_{50}/MIC_{90}) of ≥64 (Figure 1C). Additionally, chlorflavonin also inhibited growth of all four tested *M. tuberculosis* XDR clinical isolates with similar potency as compared to H37Rv (Figure 1D), implying that this compound inhibits targets which are not affected by resistance mechanisms to clinical drugs in XDR strains. In contrast, the growth of the fast growing nosocomial bacteria *Staphylococcus aureus*, *Enterococcus faecium*, and *Acinetobacter baumannii* was not inhibited in complex (Müller-Hinton broth) or minimal medium (M9 medium). Therefore, chlorflavonin displays a highly specific and selective antitubercular activity.

***In Vitro* Killing Kinetics.** Killing kinetics were performed to reveal whether chlorflavonin exerts a bacteriostatic or bactericidal effect. Chlorflavonin showed a bacteriostatic effect that was stable over a period of 3 weeks without triggering the

DOI: 10.1021/acsinfecdis.7b00055
ACS Infect. Dis. 2018, 4, 123–134

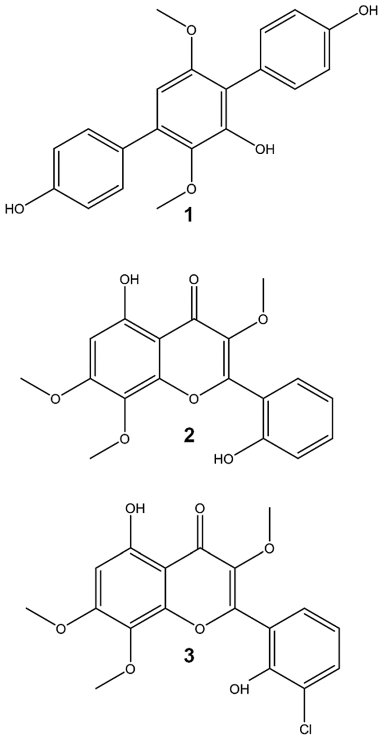

Figure 2. Chemical structures of terphenyllin (**1**), dechlorflavonin (**2**), and chlorflavonin (**3**).

outgrowth of spontaneous resistant mutants when using a starting inoculum of 10^6 CFU/mL (Figure 3A). This contrasts with the tested clinical anti-TB drugs isoniazid, rifampicin, ethambutol, bedaquiline, and delamanid, which all exhibited limited killing capacity to various degrees but resulted in outgrowth of cells after 3 to 4 weeks of treatment, which might be due to replication of resistant mutants or due to consumption or degradation of drugs allowing the surviving cells to resume growth (Figure 3B–F). Due to the fact that chemotherapy against TB relies on combined drug regimens, the individual interaction of chlorflavonin with the aforementioned clinical drugs was assessed. Addition of chlorflavonin resulted in what appeared to be additive effects with rifampicin, ethambutol, and bedaquiline in this assay, slightly enhancing the bactericidal effect of these compounds and effectively preventing the rapid emergence of resistant mutants that was seen when treating *M. tuberculosis* in monotherapy with these drugs (Figure 3B–D). Interestingly, however, the combination of isoniazid or delamanid with chlorflavonin, respectively, revealed a pronounced synergistic killing effect, resulting in the complete sterilization of the culture after 3 weeks (isoniazid, Figure 3E) or even 1 week (delamanid, Figure 3F).

The different levels of drug interactions (apparent additive vs synergistic effects as suggested by the time-kill assays) were also evaluated in a checkerboard assay by determining the fractional inhibitory concentration indices (FICI) for a combination of chlorflavonin with rifampicin or delamanid, respectively. Presence of rifampicin at 0.5 × MIC (0.078 μM) strongly increased sensitivity toward chlorflavonin (≥256-fold reduction in MIC), revealing a partial synergistic effect (FICI ≤ 0.504). Likewise, presence of delamanid at 0.5 × MIC (0.293 μM) strongly increased sensitivity toward chlorflavonin (≥256-fold reduction in MIC), whereas synergism was observed for a combination of 0.391 μM chlorflavonin and 0.146 μM delamanid (FICI = 0.5) (Table S2). The molecular basis of this exceptionally potent, yet unexpected, bactericidal interaction of chlorflavonin with delamanid and isoniazid is elusive. However, it is interesting to note that isoniazid and delamanid are both prodrugs that inhibit mycolic acid biosynthesis,[18] implicating that this pathway might become particularly vulnerable in the presence of chlorflavonin. In summary, although only possessing bacteriostatic properties in monotherapy and thus appearing less attractive compared to bactericidal drug candidates, these findings suggest that chlorflavonin could be a highly beneficial component of first- and second-line treatment regiments for suppressing resistance development and shortening of treatment durations.

Mode-of-Action and Resistance Mechanism. Chlorflavonin has previously been reported to inhibit growth of selected fungal species.[19] However, the molecular mechanisms underlying this antifungal activity have not been revealed. In order to gain insights into the mode-of-action of chlorflavonin and the molecular target(s) as well as into possible mechanisms of resistance in *M. tuberculosis*, spontaneous resistant mutants were isolated on solid medium containing 10 μM chlorflavonin, which occurred at a frequency of 10^{-7} and exhibited high-level resistance (>16-fold shift in MIC) (Figure 4A). To identify the resistance-mediating mutations, genomic DNA was isolated from five independent mutants and subjected to whole-genome resequencing. All analyzed mutants harbored single nucleotide polymorphisms (SNPs) giving rise to various nonsynonymous mutations in the gene *ilvB1* (Rv3003c) encoding the catalytic subunit of the acetohydroxyacid synthase (AHAS). Three mutants harbored additional single nucleotide polymorphisms, which were all in different loci and thus appear unrelated to resistance (Table 1).

The common mutations in *ilvB1* pointed toward a specific role of the encoded protein in chlorflavonin resistance and action. AHAS, composed of the catalytic subunit IlvB1 and the regulatory subunit IlvN, mediates the first step in branched-chain amino acid biosynthesis by catalyzing the condensation of two molecules of pyruvate to acetolactate with release of CO_2, giving rise to the amino acids leucine and valine after further metabolism. In addition, AHAS also catalyzes the condensation of pyruvate and α-ketobutyrate to acetohydroxybutyrate with release of CO_2, giving rise to the amino acid isoleucine after further metabolism.[20] Furthermore, an intermediate in the pathway for leucine and valine formation downstream of acetolactate, α-ketoisovalerate, is also the precursor for biosynthesis of pantothenic acid[21] (Figure 4B). We therefore hypothesized that chlorflavonin, through inhibition of IlvB1, might block the *de novo* biosynthesis of leucine, valine, isoleucine, and pantothenic acid, causing combined auxotrophies and growth restriction of *M. tuberculosis* during cultivation in a defined medium such as Middlebrook 7H9. Indeed, supplementation of the medium with leucine, valine, isoleucine, and pantothenic acid (at concentrations of 50 mg/L each), but not the addition of the single components (isoleucine, leucine + valine, pantothenic acid), completely reversed the inhibitory effect of chlorflavonin on *M. tuberculosis*, while omission of pantothenic acid resulted only in partial reversal of susceptibility (Figure 4C). These findings demonstrate that the antibacterial effect of chlorflavonin is highly likely mediated through inhibiting enzymatic activity of AHAS and that chlorflavonin specifically inhibits AHAS without causing any off-target effects in *M. tuberculosis* relevant for its antibacterial properties.

DOI: 10.1021/acsinfecdis.7b00055
ACS Infect. Dis. 2018, 4, 123–134

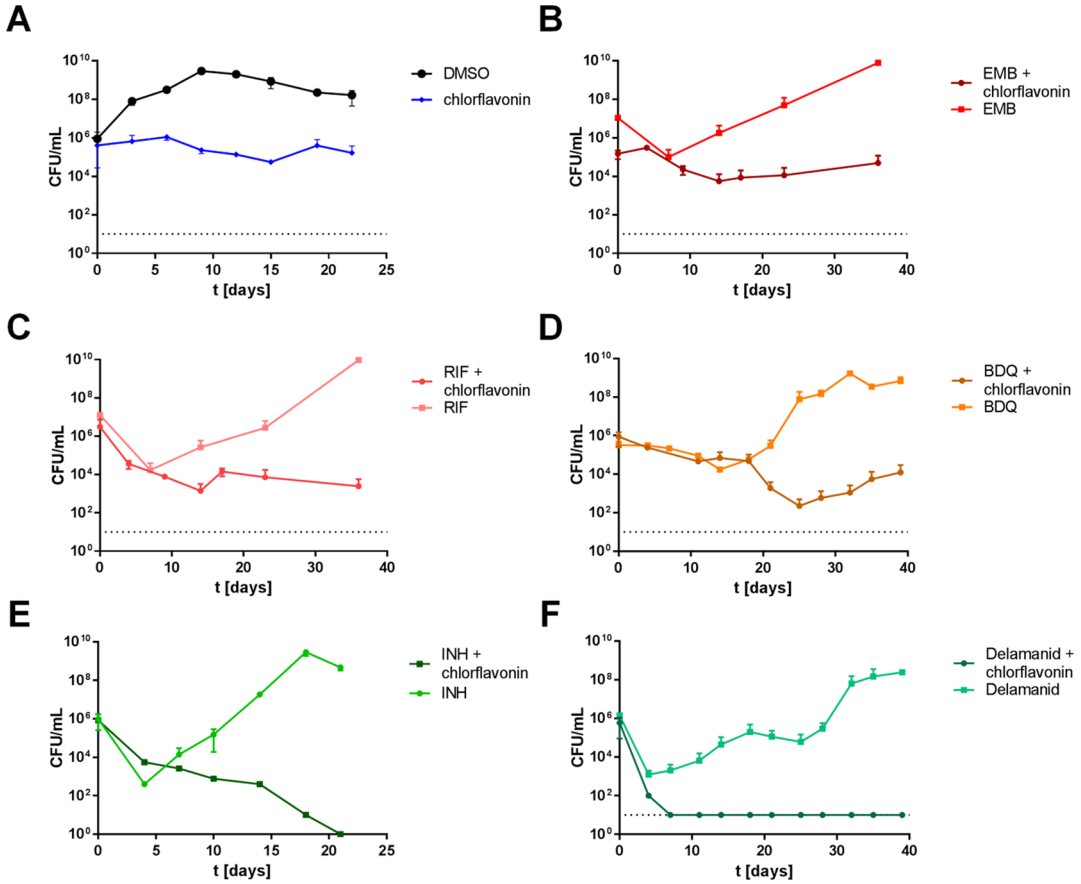

Figure 3. Time-killing curves of *M. tuberculosis* H37Rv in chlorflavonin−clinical drug combination treatments. (A) 10 μM chlorflavonin (blue ●) and solvent control 0.1% DMSO (black ●); (B) 10 μM ethambutol (EMB) (red ■) and combination of 10 μM EMB and 10 μM chlorflavonin (maroon ●); (C) 1 μM rifampicin (RIF) (peach ■) and combination of 1 μM RIF and 10 μM chlorflavonin (light red ●); (D) 0.5 μM bedaquiline (BDQ) (dark yellow ■) and combination of 0.5 μM BDQ and 10 μM chlorflavonin (light brown ●); (E) 10 μM isoniazid (INH) (light green ●) and combination of 10 μM INH and 10 μM chlorflavonin (dark green ■); (F) 0.5 μM delamanid (blue−green ■) and combination of 0.5 μM delamanid and 10 μM chlorflavonin (dark green ●). Limit of detection (indicated by the dotted line) was 10 colony forming units (CFU)/mL in all experiments except for E where the limit of detection was 1 CFU/mL. Data are means of duplicate measurements. Experiments have been repeated once with similar results.

On the basis of available crystal structures of AHAS proteins from *Arabidopsis thaliana* and *Saccharomyces cerevisiae* (PDB IDs 1YBH and 1T9C), a homology model of *M. tuberculosis* IlvB1 was generated (sequence identities of 45% and 44%; the template structures are in the bound state). Molecular docking was performed using Glide to unravel how chlorflavonin might interact with IlvB1. The protein and ligand preparation as well as the docking parameters were validated by initially redocking the known inhibitory ligand sulfometuron methyl to the acetohydroxyacid synthase structure of *S. cerevisiae* (PDB ID 1T9C).[22] The binding mode generated by Glide with the lowest energy deviated from the crystallized binding mode by 0.3 Å, demonstrating a very good docking result (Figure S8A). Applying the same docking parameters, docking of chlorflavonin in IlvB1 yielded three binding modes that differed by 3.7, 6.7, and 8.2 Å (Figure S8B). In order to identify which of these is most likely, we also docked chlorflavonin into IlvB1 using AutoDock3.0/DrugScore as docking engine/objective function combination. This docking identified one binding mode that deviates by only 0.2 Å from one generated by Glide (Figure 5A). Overall, both docking results showed that chlorflavonin can bind into the putative active site of the enzyme, where it forms a hydrogen bond and a salt bridge with lysine 197, a hydrogen bond with the backbone of phenylalanine 147, a $\pi-\pi$ interaction between the phenyl moiety and tryptophan 516, and a cation$-\pi$ interaction between the chromenyl moiety and arginine 318 (Figure 5B). The chlorine atom points into a subpocket lined by leucine 65 (chain A), methionine 512, and valine 513; apparently, the chlorine atom acts as a lipophilic appendage to fill the hydrophobic subpocket, which may lead to a higher binding affinity compared to the dechloro derivative. In addition to lysine 197, other residues observed in resistance mutations, i.e., glycine 62 and alanine 63, are also part of, or in close proximity to, respectively, the putative active site. Overall, these findings suggest that chlorflavonin likely impairs entry of the natural substrates pyruvate and α-ketobutyrate to the putative active site. Mutations of certain amino acids in the active site likely mediate resistance by preventing binding of chlorflavonin without substantially affecting normal enzymatic activity.

Expression, Purification, and *in Vitro* Activity of IlvB1. Since the molecular docking studies did not reveal a definitive role of the chlorine atom in interaction of chlorflavonin with IlvB1, this raised the question of why dechlorflavonin does not possess antimycobacterial activity against whole cells. To corroborate direct target engagement and to determine the importance of chlorination for inhibition of enzymatic activity, the catalytic subunit IlvB1 and the mutated variant IlvB1-

DOI: 10.1021/acsinfecdis.7b00055
ACS Infect. Dis. 2018, 4, 123−134

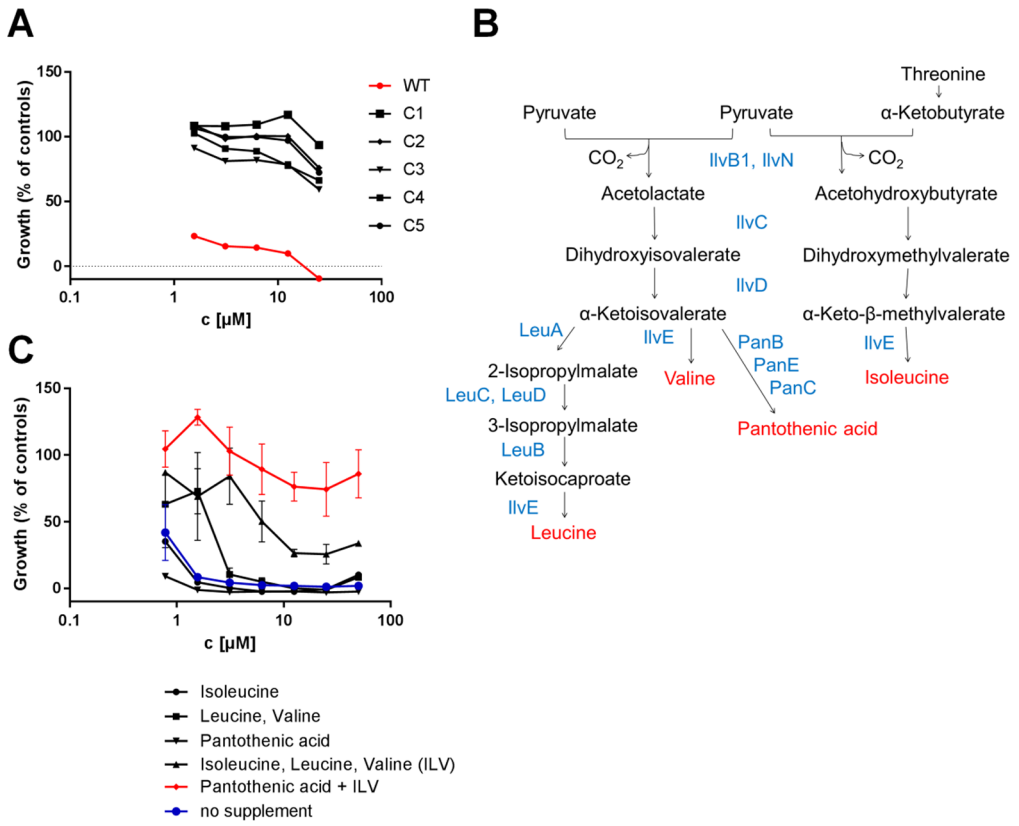

Figure 4. Chlorflavonin blocks biosynthesis of branched-chain amino acids and pantothenic acid through inhibition of the catalytic subunit of acetohydroxyacid synthase, IlvB1. (A) Dose−response curves of chlorflavonin-resistant *M. tuberculosis* H37Rv mutants. Growth was quantified using the resazurin dye reduction assay. Data represent single measurements. (B) Pathway for biosynthesis of branched-chain amino acids and pantothenic acid in *M. tuberculosis* and role of acetohydroxyacid synthase IlvB1-IlvN. (C) Supplementation with branched-chain amino acids and pantothenic acid (50 mg/L each) abrogates sensitivity of *M. tuberculosis* to chlorflavonin. Growth was quantified using the resazurin dye reduction assay. Data are means of triplicates ± SD.

Table 1. Mutations in Chlorflavonin-Resistant *M. tuberculosis* H37Rv Mutants Identified by Whole-Genome Sequencing

chlorflavonin-resistant mutant	mutation(s) gene: amino acid substitution	nucleotide substitution in *ilvB1* gene
C1	*ilvB1*: G62S, *mmpL 11*: E667A	G184A
C2	*ilvB1*: K197T, *alkB*: M248T	A590C
C3	*ilvB1*: G62S	G184A
C4	*ilvB1*: A63V	C188T
C5	*ilvB1*: K197R, Rv1990A: E40K	A590G

K197T from *M. tuberculosis* were recombinantly expressed in *E. coli* as N-terminal hexahistidine-tagged proteins (68.3 kDa), which were partially purified employing Ni-NTA (nitrilotriacetic acid) affinity chromatography and desalted by gel filtration (Figure 6A). The partially purified IlvB1 preparation displayed AHAS activity as demonstrated by red complex formation which developed linearly under the tested assay conditions over at least 1 h. Also, the mutated enzyme carrying an amino acid substitution found in one of the spontaneous resistant mutants, K197T, displayed normal AHAS activity (Figure 6B). AHAS activity was strongly inhibited in the presence of chlorflavonin only in case of the wild-type, but not of the mutated, IlvB1 (Figure 6C), corroborating target engagement and direct interaction of the compound with IlvB1 as suggested by the molecular docking studies. Furthermore, this supports the proposed mode of resistance with certain amino acid substitutions in or near the active site of the enzyme preventing binding of chlorflavonin without impairing regular activity. The inhibitory effect of chlorflavonin against the catalytic subunit of AHAS was even stronger than for the known IlvB1 inhibitor pyrazosulfuron ethyl (PSE)[23] (Figure 6C). Interestingly, dechlorflavonin impaired AHAS catalytic activity only slightly at a high dose of 50 μM, demonstrating that chlorination is indeed critical for compound−target interaction and providing an explanation for the differing antibacterial whole-cell effect of chlorflavonin and dechlorflavonin (Figure 6C).

Intracellular Activity in Infected Macrophages. Since *M. tuberculosis* is an intracellular pathogen largely residing within arrested phagolysosomes of infected macrophages, the intracellular activity of antibiotics plays an important role for the treatment of TB. Thus, a human THP-1 macrophage infection model was employed to investigate whether chlorflavonin is able to penetrate into macrophage cells and influence the intracellular growth of phagocytosed bacteria. In this experiment, reporter strains of *M. tuberculosis* H37Rv wild-type and of the chlorflavonin-resistant mutant C4, both expressing the red fluorescent mCherry protein constitutively from an episomal plasmid, were employed for macrophage infection. As indicated by the reduced amount of integrated density of mCherry fluorescence down to 1.4% compared to untreated controls, chlorflavonin at a concentration of 10 μM clearly inhibited intracellular growth of *M. tuberculosis* wild-type cells. Intracellular activity was less pronounced compared to the

DOI: 10.1021/acsinfecdis.7b00055
ACS Infect. Dis. 2018, 4, 123−134

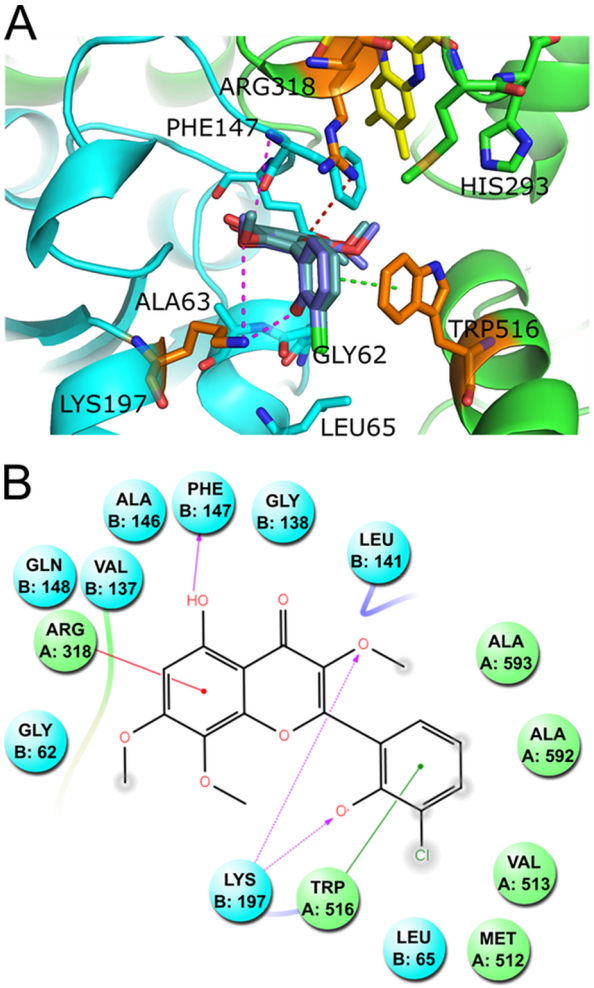

Figure 5. Interaction of chlorflavonin with IlvB1. A computational homology model of *M. tuberculosis* H37Rv IlvB1 was constructed using AHAS proteins from *Saccharomyces cerevisiae* and *Arabidopsis thaliana* (PDB ID 1T9C and 1YBH) as templates. (A) Binding mode of chlorflavonin (highlighted in blue and violet) in the putative active site identified by docking with Glide (blue) and AutoDock (violet). Chain A is represented in green and chain B, in cyan. (B) 2D view of potential amino acid residues interacting with chlorflavonin. "A" and "B" are protein chain identifiers.

first-line antibiotics rifampicin (3 μM) and isoniazid (5 μM) but superior to streptomycin (20 μM). Additionally, the combination of INH and chlorflavonin had a stronger effect than INH alone (Figure 7A,C), suggesting that both compounds might also work synergistically in an intracellular infection context. In contrast, the chlorflavonin-resistant *M. tuberculosis* mutant reporter strain was not inhibited by chlorflavonin, whereas susceptibility to the other antibiotics was not affected by the *ilvB1* mutation in this resistant clone (Figure 7B,C). This demonstrates that chlorflavonin can penetrate mammalian host cells, reaches *M. tuberculosis* within its intracellular compartment, and exhibits antibacterial activity in an IlvB1-dependent manner. *M. tuberculosis* is obviously unable to acquire branched-chain amino acids or pantothenic acid from the human host cells to a significant extent, which would otherwise compensate for the effect of chlorflavonin.

This study identified chlorflavonin as a promising novel lead structure for TB chemotherapy due to its high antibacterial potency, lack of cytotoxicity, high selectivity, and intracellular activity in infected macrophages. We could show that chlorflavonin inhibits the biosynthesis of the branched-chain amino acids isoleucine, leucine, and valine as well as of pantothenic acid in *M. tuberculosis* and causes combined auxotrophies. Leucine and pantothenic acid auxotrophic mutants of *M. tuberculosis* are highly attenuated in different animal models,[24−27] indicating that *M. tuberculosis* cannot acquire these metabolites from the host during infection. Thus, targeting biosynthesis of branched-chain amino acids and pantothenic acid via inhibition of AHAS is a valid approach to restrict growth of *M. tuberculosis in vivo*, which is further supported by the clear IlvB1-dependent activity of chlorflavonin in human THP-1 macrophages. The specificity of chlorflavonin for the IlvB1 subunit of AHAS explains the lack of cytotoxicity because this protein is absent from mammals, which are unable to synthesize branched-chain amino acids as well as pantothenic acid *de novo* and rely on uptake of these essential nutrients from their diet. An *ilvB1* gene deletion mutant of *M. tuberculosis*, that is viable in the presence of branched-chain amino acids, was recently reported to be only moderately attenuated in mice and fully virulent in murine bone marrow-derived macrophages,[28] suggesting that specific inhibition of IlvB1 might have limited therapeutic potential. However, three different *ilvB1* homologues are encoded in the *M. tuberculosis* genome (*ilvB2*, *ilvG*, and *ilvX*), which might possess at least partial functional redundancy.[29] While IlvB1 is essential for growth *in vitro* in absence of branched-chain amino acids,[28] one or more of the three isoforms might be expressed during growth in murine macrophages or mice to compensate for loss of IlvB1. However, since all isoforms are similar and probably share a common catalytic mechanism, it is likely that chlorflavonin can also inhibit the other AHAS isoforms.

In addition to bacteria, AHAS is also found in plants and fungi. In fact, commercially marketed herbicides belonging to the classes of sulfonylurea,[30] imidazolinones,[31] pyrimidinyl thiobenzoates, and triazolopyrimidine sulphonamides are known to be potent inhibitors of plant AHAS. There is a growing number of recent studies demonstrating antibacterial activity of members of these herbicide classes against *M. tuberculosis*.[23,32−37] In 1998, it was shown that the commercial AHAS inhibitor sulfometuron methyl inhibited *M. tuberculosis* growth in a mouse infection model, albeit having just a moderate effect only at a high daily dosage.[38] However, recently, some monosubstituted sulfonylurea derivatives were shown to be more active in mice capable of significantly reducing lung burden after *M. tuberculosis* infection, including infection with an XDR-TB strain.[34] These examples highlight the great therapeutic potential of AHAS inhibitors and promise that chlorflavonin could exhibit considerable potency in animal models. Chlorflavonin is structurally unrelated to the before mentioned molecules and thus represents a novel class of AHAS inhibitors.

MATERIAL AND METHODS

General Analytical Procedures. ^{1}H, ^{13}C, and 2D NMR spectra were recorded at 25 °C in DMSO-d_6 on a Bruker ARX 600 NMR spectrometer. Chemicals shifts were referenced to the solvent residual peaks, δ_H 2.50 for ^{1}H and δ_C 39.5 for ^{13}C NMR. Mass spectra (ESI) were recorded with a Finnigan LCQ Deca mass spectrometer, and HRMS (ESI) spectra were obtained with a FTHRMS-Orbitrap (Thermo-Finnigan) mass spectrometer. Solvents were distilled prior to use, and spectral grade solvents were used for spectroscopic measurements.

DOI: 10.1021/acsinfecdis.7b00055
ACS Infect. Dis. 2018, 4, 123−134

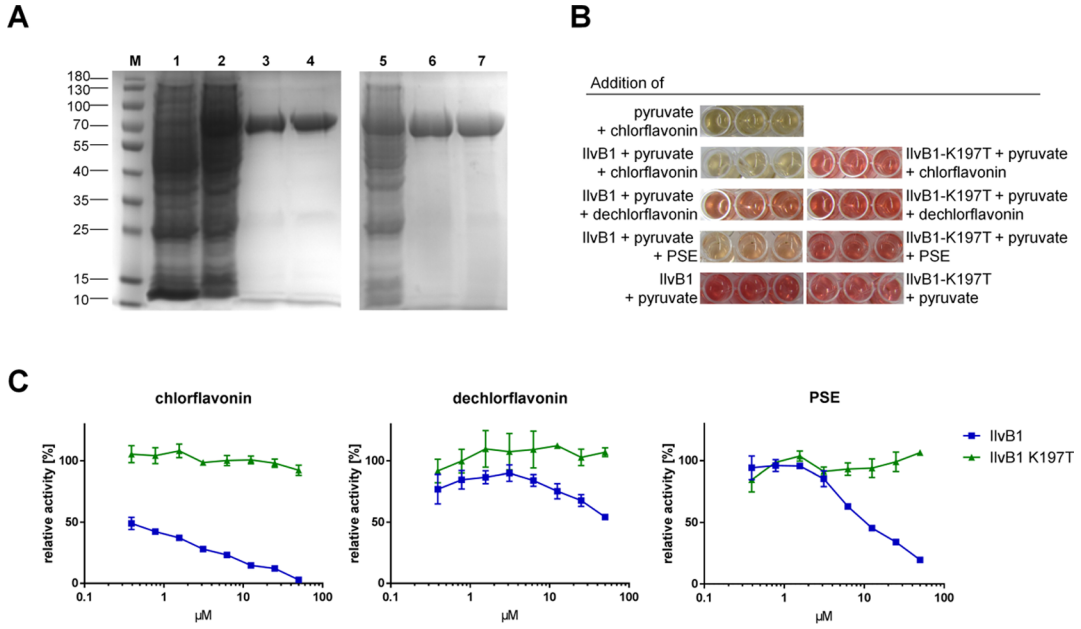

Figure 6. Purification and activity assay of recombinant IlvB1-His6. (A) SDS-PAGE analysis of Ni-NTA purification employing crude extracts of induced cells of *E. coli* Rosetta (DE3) pLysS harboring pET30a::*ilvB1*-His6 or pET30a::*ilvB1*-K197T-His6 expression plasmid. 12% polyacrylamide gel was used, and proteins were stained with Coomassie. Lane M: protein marker ranging from 10 to 180 kDa; lane 1: crude extract *E. coli* pET30a; lane 2: crude extract *E. coli* pET30a::*ilvB1*-His6; lane 3: IlvB1-His6 protein after Ni-NTA chromatography; lane 4: IlvB1-His6 protein after desalting; lane 5: crude extract *E. coli* pET30a::*ilvB1*-K197T-His6; lane 6: IlvB1-K197T-His6 protein after Ni-NTA chromatography; lane 7: IlvB1-K197T-His6 protein after desalting. (B, C) Inhibition of recombinant IlvB1-His6 or IlvB1-K197T-His6 (each at 2.5 μg/mL) by chlorflavonin, dechlorflavonin, or pyrazosulfuron ethyl (PSE). All experiments were performed according to Choi et al.[23] using reaction buffer (100 mM K_3PO_4, pH 7.5, 10 mM $MgCl_2$, 1 mM thiamine diphosphate, 50 μM FAD) and 75 mM pyruvate as substrate with the listed additional compounds and incubated for 1 h at 37 °C. IlvB1 activity was demonstrated by formation of a red complex (B) which was quantitatively measured by absorbance at 492 nm using a microplate reader (C). Activities in (C) were calculated as percentage of uninhibited enzyme control and are displayed as mean of triplicates ± SD.

HPLC analysis was performed with a Dionex UltiMate3400 SD machine with a LPG-3400SD Pump coupled to a photodiode array detector (DAD3000RS); routine detection was set at 235, 254, 280, and 340 nm. The separation column (125 mm × 4 mm) was prefilled with Eurosphere-10 C18 (Knauer, Germany), and the following gradient was used (MeOH, 0.1% HCOOH in H_2O): 0 min (10% MeOH), 5 min (10% MeOH), 35 min (100% MeOH), and 45 min (100% MeOH). Semipreparative HPLC was performed using a Merck Hitachi HPLC System (UV detector L-7400; Pump L-7100; Eurosphere-100 C18, 300 mm × 8 mm, Knauer, Germany). Column chromatography included LH-20 Sephadex and Merck MN Silica gel 60 M (0.04−0.063 mm). TLC plates with silica gel F254 (Merck, Darmstadt, Germany) were used to monitor fractions (CH_2Cl_2/MeOH mixtures as mobile phase); detection was under UV at 254 and 366 nm or by spraying the plates with anisaldehyde reagent.

Fungal Material. *Mucor irregularis* was isolated from fresh healthy leaves of *Moringa stenopetala* (Moringaceae) collected in Koukoue, Littoral region, Cameroon in July 2013. The fungus was isolated under sterile conditions from the inner tissue of the leaf according to the procedure described by Kjer et al.[39] The identification was performed following a molecular biological protocol by DNA amplification and sequencing of the ITS region. The sequence data have been submitted to GenBank, accession number KP067786.

Fermentation, Extraction, and Isolation. Fermentation of the fungus was carried out in two flasks (1 L each). The fungus was grown on rice medium (to 100 g of commercially available rice, 110 mL of distilled water was added and kept overnight prior to autoclaving), at room temperature under static conditions for 40 days. After incubation, each fungal culture was extracted with EtOAc (3 × 250 mL). The obtained EtOAc extract (856.0 mg) was partitioned between *n*-hexane and 90% MeOH. The 90% MeOH fraction labeled AST-53 (598.4 mg) was subjected to vacuum liquid chromatography (VLC) on silica gel employing a step gradient of hexane−EtOAc and dichloromethane−methanol to give six fractions AST-53-A to AST-53-F. Fraction AST-53-A (40% hexane in EtOAc, 58.2 mg) was subjected to column chromatography over Sephadex LH-20 using MeOH as eluent to give three subfractions AST-53-A1 to AST-53-A3. Subfraction AST-53-A2 (27 mg) was further purified by semipreparative HPLC using a gradient of MeOH−H_2O (0.1%TFA), to afford compounds **1** (2 mg), **2** (3 mg), and **3** (9 mg).

Bacterial Strains and Growth Conditions. Cells of *M. tuberculosis* H37Rv and of several XDR-TB clinical isolates from South Africa[40] were grown aerobically in Middlebrook 7H9 medium supplemented with 10% (v/v) ADS enrichment (5%, w/v, bovine serum albumin fraction V; 2%, w/v, glucose; 0.85%, w/v, sodium chloride), 0.5% (v/v) glycerol, and 0.05% (v/v) tyloxapol at 37 °C. Hygromycin (50 mg/L) was added for selection for reporter strains. XDR-TB clinical strains originating from South Africa were obtained from William. R. Jacobs Jr. (Albert Einstein College of Medicine, Bronx, USA) and exhibited the following resistances: 1 mg/L isoniazid, 1 mg/L rifampicin, 10 mg/L ethambutol, 2 mg/L streptomycin, 100 mg/L pyrazinamide, 5 mg/L ethionamid, 5 mg/L kanamycin, 4 mg/L amikacin, 10 mg/L capreomycin, and 2 mg/L ofloxacin.

Nosocomial bacterial strains were cultivated in Müller Hinton (MH) medium at 37 °C and included *Staphylococcus*

DOI: 10.1021/acsinfecdis.7b00055
ACS Infect. Dis. 2018, 4, 123−134

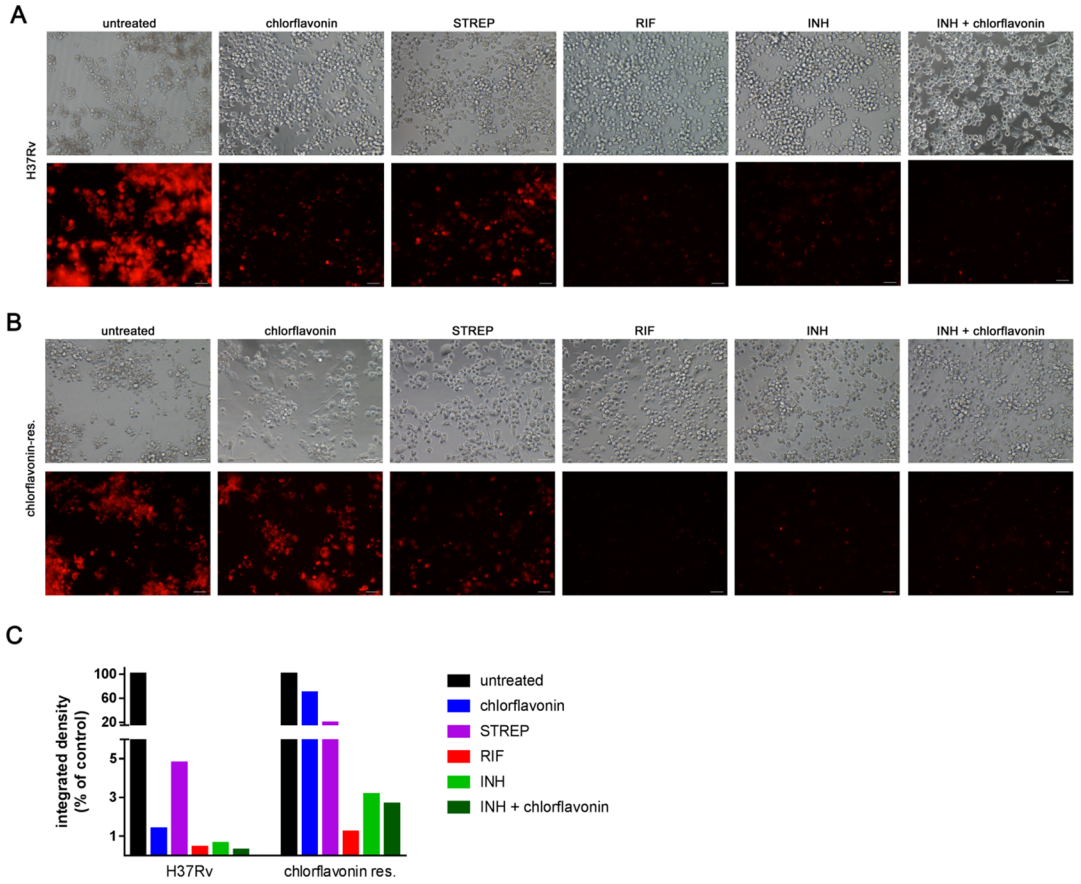

Figure 7. Intracellular activity of chlorflavonin in a THP-1 macrophage infection model. THP-1 cells were infected with a mCherry expressing reporter strain of either *M. tuberculosis* H37Rv wild-type (A) or a chlorflavonin-resistant mutant (B) in a 96-well microtiter plate and subjected to different antibiotic treatments as indicated. THP-1 cells were infected for 3 h, washed with PBS to remove unphagocytosed bacteria, and treated with 10 μM chlorflavonin, 20 μM streptomycin (STREP), 3 μM rifampicin (RIF), 5 μM isoniazid (INH), or 5 μM isoniazid and 10 μM chlorflavonin (INH + chlorflavonin) as indicated. After 5 days postinfection, wells were imaged using a fluorescence microscope with extinction wavelength of 560 nm, 200× magnification, and 1.5 s exposure time; scale bars: 50 μm. (C) Integrated density of red fluorescence as percent of untreated control of *M. tuberculosis* H37Rv WT and chlorflavonin resistant mutant, respectively, calculated with ImageJ.

aureus: MSSA strain ATCC 25923, MRSA/VISA ATCC 700699; *Entercoccus faecalis*: ATCC 29212, ATCC 51299 (vancomycin resistant); *Enterococcus faecium*: ATCC 35667, ATCC 700221 (vancomycin resistant); *Acinetobacter baumannii*: ATCC BAA 1605 (multidrug resistant).

Determination of Minimal Inhibitory Concentration (MIC) against *M. tuberculosis* via Resazurin Dye Reduction Method. For the determination of MIC against *M. tuberculosis*, bacteria were precultured until log phase ($OD_{600\ nm}$ = 0.5−1) and then seeded at 1×10^5 cells per well in a total volume of 100 μL in 96-well round-bottom microtiter plates and incubated with 2-fold serially diluted extracts or compounds at a concentration range of 100−0.78 μg/mL or μM, respectively. Microplates were incubated at 37 °C for 5 days. Afterward, 10 μL/well of a 100 μg/mL resazurin solution was added and the plates were incubated at ambient temperature for a further 16 h. Then, cells were fixed for 30 min after formalin addition (5%, v/v, final concentration). For viability determination, fluorescence was quantified using a microplate reader (excitation of 540 nm, emission of 590 nm). Percentage of growth was calculated relative to rifampicin treated (0% growth) and DMSO treated (100% growth) controls.

Determination of MIC against Nosocomial Strains. MIC of chlorflavonin for various typical nosocomial bacterial pathogens (*Staphylococcus aureus, Enterococcus faecalis, Enterococcus faecium, Acinetobacter baumannii*) was determined by the broth microdilution method according to the recommendations of the Clinical and Laboratory Standards Institute (CLSI).[41] For preparation of the inoculum, the growth method was used. Bacterial cells were grown aerobically in MH medium at 37 °C and 180 rpm. A preculture was grown until log phase ($OD_{600\ nm} \sim 0.5$) and then seeded at 5×10^4 bacteria/well in a total volume of 100 μL in 96-well round-bottom microtiter plates and incubated with a 2-fold serially diluted compound at a concentration range of 100−0.78 μM. Microplates were incubated aerobically at 37 °C for 24 h. MIC was determined by identifying the minimum concentration of the compound that led to complete inhibition of visual growth of the bacteria. To test efficacy of chlorflavonin not only in complex MH medium but also in a defined mineral salts medium, the same experiment was performed in M9 medium (1× M9 salts, 2 mM $MgSO_4$, 0.1 mM $CaCl_2$, 1% glucose, 0.05 mM nicotinamide, 0.03−1% casamino acids). For each strain, the minimal amount of casamino acids for supporting normal growth was determined, thereby avoiding oversupplemenation of cells with branched-chain amino acids which might mask the effect of chlorflavonin (*Staphylococcus aureus* MSSA strain ATCC 25923: 0.25%, MRSA/VISA ATCC 700699: 0.125%; *Enterococcus faecalis* ATCC 29212: 1%, ATCC 51299 (vancomycin

DOI: 10.1021/acsinfecdis.7b00055
ACS Infect. Dis. 2018, 4, 123−134

resistant): 0.25%; *Enterococcus faecium* ATCC 35667: 1%, ATCC 700221 (vancomycin resistant): 0.25%; *Acinetobacter baumannii* ATCC BAA 1605: 0.06% of casamino acids). The precultures were washed with PBS, resuspended in M9, and tested for susceptibility as described before.

Determination of Cytotoxicity and Therapeutic Index. The cytotoxicity of chlorflavonin was determined *in vitro* using the human monocyte cell line THP-1 (Deutsche Sammlung von Mikroorganismen and Zellkulturen GmbH) and the human fetal lung fibroblast cell line MRC-5 (American Type Culture Collection). THP-1 cells were cultured in RPMI 1640 medium containing 10% (v/v) fetal bovine serum (FBS), while MRC-5 cells were incubated in Dulbecco's Modified Eagles Medium (DMEM) containing 10% (v/v) FBS both at 37 °C in a humidified atmosphere of 5% CO_2. Cells were seeded at approximately 5×10^4 cells/well in a total volume of 100 μL in 96-well flat bottom microtiter plates containing a 2-fold serially diluted compound at a maximum final concentration of 100 μM. Cells treated with DMSO in a final concentration of 1% (v/v) served as solvent controls. After an incubation time of 48 h, 10 μL of resazurin solution (100 μg/mL) was added per well and incubated for a further 3 h at 37 °C in a humidified atmosphere of 5% CO_2. Fluorescence was quantified using a microplate reader (excitation of 540 nm, emission of 590 nm). Growth was calculated relative to noninoculated (i.e., cell-free) (0% growth) and untreated (100% growth) controls in triplicate experiments, respectively. For determination of the therapeutic index of the substance, the selectivity index (SI) was determined by the quotient of cytotoxic concentration and MIC.

Determination of Time-Kill Curves *in Vitro*. Bacteria cells were grown aerobically at 37 °C in 10 mL Middlebrook 7H9 liquid media supplemented with 0.5% (v/v) glycerol, 0.05% (v/v) tyloxapol, and 10% (v/v) ADS enrichment as shaking cultures. Exponentially growing cultures were diluted to a titer of ca. 1×10^6 CFU/mL as estimated from optical density measurement based on the calculation that an $OD_{600\ nm}$ of 1 translates into 3×10^8 CFU/mL. Chlorflavonin was added at a concentration of 10 μM ($3.2 \times MIC_{100}$) either alone or in individual combination with clinical drugs (1 μM rifampicin, 10 μM isoniazid, 10 μM ethambutol, 0.5 μM bedaquiline, 0.5 μM delamanid). Culture aliquots were taken at different time points, and 10-fold serial dilutions were plated on Middlebrook 7H10 agar plates to count viable cells after 3 weeks of incubation at 37 °C.

Checkerboard Synergy Assay. The fractional inhibitory concentration index (FICI) of chlorflavonin with isoniazid, delamanid, or rifampicin, respectively, was determined in a 96-well plate format employing 2-dimensional dilutions of compounds. *M. tuberculosis* H37Rv strain was seeded at 10^5 CFU/well in a total volume of 100 μL and incubated at 37 °C for 5 days. For quantification, the resazurin assay was used as described above. The FICI was calculated as the sum of the quotients of the lowest inhibitory concentration in a row (*A* and *B*, respectively) and the MIC of the compound (MIC_A and MIC_B, respectively):

$$\mathrm{FICI} = \frac{A}{\mathrm{MIC_A}} + \frac{B}{\mathrm{MIC_B}}$$

Total synergism (FICI $\leq$ 0.5), partial synergism (0.5 < FICI $\leq$ 0.75), no effect (0.75 < FICI $\leq$ 2), or antagonism (FICI > 2) between chlorflavonin and the tested antibiotics were deduced from the observed FICI values.[42]

Expression and Purification of Catalytic Subunit of AHAS. The catalytic subunit of AHAS from *M. tuberculosis* H37Rv was amplified by PCR using the primers 5′-TTTTT-CATATGCACCATCATCATCATCATAGCGCACC-AACCAAGCCACAC-3′ and 5′-TTTTTAAGCTTTCAGG-CGTGGCCTTCGGTGATGTC-3′ introducing an N-terminal hexahistidine tag (IlvB1-His6) and ligated into a pET30a vector using the restriction sites *Nde*I and *Hin*dIII (underlined). The mutated IlvB1 enzyme with the amino acid substitution K197T was generated by mutagenesis PCR using the primers 5′-GACATCCCCACGGACGTGCTGCAGG-3′ and 5′-GACCA-GCACCGCGCCCGG-3′ employing the Q5 site directed mutagenesis kit (NEB).

The plasmids were transformed into *E. coli* Rosetta (DE3) pLysS. The recombinant cells were cultivated with 40 μg/mL kanamycin and 10 μg/mL chloramphenicol until the culture reached an OD at 600 nm of 0.8. The expression of the recombinant proteins was induced by adding 0.5 mM isopropyl-β-D-thiogalactopyranoside (IPTG) and subsequent incubation overnight at room temperature. Bacteria were pelleted at 4000 rpm for 30 min, and the 1 mg pellet was suspended in 5 mL of buffer A (20 mM sodium phosphate, pH 8.0; 0.5 M NaCl and 20 mM imidazole) containing protease inhibitor cocktail. Afterward, the cells were lysed by bead beating and the extract was centrifuged at 14 000 rpm at 4 °C for 40 min to prepare lysates. The supernatant was loaded onto a Ni-NTA column, which was equilibrated with buffer A. The column was washed with buffer A thoroughly. Subsequently, the bound proteins were eluted with elution buffer (20 mM sodium phosphate, pH 8.0; 0.5 M NaCl and 500 mM imidazole). Size exclusion chromatography for desalting was performed on a PD MidiTrap G-25 (GE Healthcare) equilibrated with 100 mM K_3PO_4, pH 7.5, containing 0.15 M NaCl.

Microplate Assay of IlvB1 Activity. IlvB1 activity was measured according to Choi et al.[23] Briefly, IlvB1 protein (2.5 μg/mL) was incubated in reaction buffer (100 mM K_3PO_4, pH 7.5, 10 mM $MgCl_2$, 1 mM thiamine diphosphate, 50 μM FAD) with 75 mM pyruvate in a total volume of 100 μL for 1 h at 37 °C, leading to acetolactate formation. Afterward, reactions were stopped by addition of 0.5 M H_2SO_4 and incubation for 15 min at 65 °C with decarboxylate acetolactate to yield acetoin. At last, 100 μL of reaction product was mixed with 90 μL of 0.5% (w/v) creatine and 90 μL of 5% (w/v) α-naphtol solution in 2.5 M NaOH, leading to formation of a red complex together with acetoin which was quantified by absorbance at 492 nm using a microplate reader. Product formation proceeded linearly for at least 1 h under the tested conditions.

Intracellular Activity Assay via Macrophage Infection. Bacterial reporter strains expressing the fluorescent mCherry protein[43] were precultured in hygromycin containing 7H9 Middlebrook medium until late log phase ($OD_{600\ nm}$ = 0.8−1). Human THP-1 cells were seeded at a density of 1×10^5 cells per well in 96-well flat bottom microtiter plates in a total volume of 100 μL of RPMI 1640 medium with stable glutamine supplemented with 10% fetal bovine serum and containing 50 nM phorbol-12-myristate-13-acetate (PMA). After 16 h of incubation at 37 °C in a humidified atmosphere of 5% CO_2, the THP-1 cells had differentiated into adherent cells with macrophage-like characteristics. The medium was replaced with 100 μL of RPMI 1640 medium without PMA containing 3×10^5 CFU per well of a reporter strain of either *M. tuberculosis* H37Rv wild-type or a chlorflavonin resistant mutant, resulting

DOI: 10.1021/acsinfecdis.7b00055
ACS Infect. Dis. 2018, 4, 123−134

in a multiplicity of infection of 3. After 3 h of infection, macrophages were washed with PBS to remove unphagocytosed bacteria, and 100 μL of RPMI 1640 medium supplemented with 10% fetal bovine serum and containing either 10 μM chlorflavonin or different antibiotics (20 μM streptomycin as negative control; 3 μM rifampicin, 5 μM isoniazid as positive controls) was added per well. After 5 days of incubation at 37 °C in a humidified atmosphere of 5% CO_2, macrophages were fixed with formaldehyde−glutaraldehyde solution (0.8% and 0.25% final concentration). Fluorescence microscopy was performed using a Nikon Eclipse TS100.

Determination of Single Step Resistance Frequency. Spontaneous resistant mutants were isolated by plating approximately 1×10^8 CFU on agar (1 mL per well in a 6-well microtiter plate) containing chlorflavonin at 4× or 5× MIC. Spontaneous resistant colonies were obtained at a frequency of ca. 1×10^{-7} after 3 weeks of incubation at 37 °C. Five independent clones were selected, which all exhibited high-level resistance against chlorflavonin in liquid culture.

Whole Genome Sequencing. To identify the resistance mediating mutations, genomic DNA of five independent mutants was isolated as described previously.[44] Libraries were prepared for sequencing using the standard paired-end genomic DNA sample prep kit from Illumina. Genomes were sequenced using an Illumina HiSeq 2500 next-generation sequencer (San Diego, CA, USA) and compared with the parent *M. tuberculosis* H37RvMA genome (GenBank accession GCA_000751615.1). Paired-end sequence data was collected with a read length of 106 bp. Base-calling was performed using Casava software, v1.8. The reads were assembled using a comparative genome assembly method, using *M. tuberculosis* H37RvMA as a reference sequence.[45] The mean depth of coverage ranged from 277× to 770 ×.

Homology Modeling. A homology model of IlvB1 (Uniprot sequence P9WG40) was generated by using the in-house tool TopModel[46,47] and the protein structure of PDB ID 1T9C of the AHAS from *S. cerevisiae* and of PDB ID 1YBH of the AHAS from *A. thaliana* as templates. 1T9C has a sequence identity (similarity) of 44% (84%) to IlvB1 and was resolved to 2.3 Å resolution, while 1YBH has a sequence identity (similarity) of 45% (84%) to IlvB1 and was resolved to 2.5 Å. The overall C_α atom root-mean-square deviation (RMSD) between the model and the template is 0.26 Å, and the RMSD of non-hydrogen atoms of the binding pocket is 1.34 Å.

Protein Structure and Ligand Preparation for Molecular Docking. The template and the homology model were both preprocessed with the Protein Preparation Wizard of the Schrödinger suite. Bond orders were assigned. Hydrogens were added; the H-bond network was optimized, and missing side chains were detected and added using Prime.[48] Finally, the systems were energy minimized using the OPLS 2005 force field, resulting in an RMSD of 0.13 Å with respect to the starting structure.[49] The structures of chlorflavonin and the cocrystallized ligand sulfometuron methyl of the template PDB ID 1T9C were sketched with ChemDraw 14. 3D structures were generated with the LigPrep module of the Schrödinger suite.

Docking with GLIDE. To validate the docking protocol, the ligand sulfometuron methyl was first redocked into the protein structure of PDB ID 1T9C using the GLIDE module[50] in standard precision (SP) mode[51] and default values for the grid generation. In a second step, the same settings for the grid generation and the GLIDE docking were used with chlorflavonin and the homology model of IlvB1. The grid had been centered on the ligand sulfometuron methyl in the binding pocket of the template PDB ID 1T9C. No restraints were used during the docking; the cocrystallized flavin-adenine dinucleotide (FAD) was kept in place. As binding mode, the docking solution with the lowest energy was chosen.

Docking with AutoDock. Docking with GLIDE led to three binding modes of chlorflavonin that differed by 3.7, 6.7, and 8.2 Å (Figure S8B). In order to identify which one of these is most likely, we docked chlorflavonin also with AutoDock3[52,53] as a docking engine, using the DrugScore[54,55] distance-dependent pair-potentials as an objective function as described in ref 56. Default values were used for the docking parameters. Docking solutions with more than 50% of all configurations in the largest cluster were considered sufficiently converged, and the configuration with the lowest docking energy of that cluster was identified as the final binding mode depicted in Figure 5.

■ ASSOCIATED CONTENT

Supporting Information

The Supporting Information is available free of charge on the ACS Publications website at DOI: 10.1021/acsinfecdis.7b00055.

Analytical data for chlorflavonin (**3**) including ^{1}H (Figure S1), ^{13}C (Figure S2), HSQC (Figure S3), HMBC (Figure S4), and ROESY (Figure S5) NMR spectra and key 2D NMR correlations of **3** (Figure S6); comparative dose−response curves for chlorflavonin (**3**), dechlorochlorflavonin (**2**), and terphenyllin (**1**) (Figure S7); docking solutions of sulfometuron methyl and chlorflavonin (Figure S8); NMR spectroscopic data of **3** (Table S1); checkerboard synergy assay (Table S2) (PDF)

■ AUTHOR INFORMATION

Corresponding Authors

*Phone: +49 211 8114180. E-mail: rainer.kalscheuer@hhu.de (R.K.).

*Phone: +49 211 8114163. E-mail: proksch@hhu.de (P.P.).

ORCID

Georgios Daletos: 0000-0002-1636-6424

Holger Gohlke: 0000-0001-8613-1447

Rainer Kalscheuer: 0000-0002-3378-2067

Author Contributions

¶N.R. and H.S.A. contributed equally. H.S.A. isolated compounds **1**−**3**, and H.S.A. and G.D. performed structural elucidation. N.R. conducted all experiments involving *M. tuberculosis* and other bacteria. G.E. and H.G. performed and analyzed molecular docking studies. T.R.I. performed and analyzed whole genome sequencing. R.K. and P.P. designed experiments and analyzed data. N.R. and R.K. wrote the manuscript with contributions and edits from all authors.

Notes

The authors declare no competing financial interest.

■ ACKNOWLEDGMENTS

R.K., H.G., and P.P. acknowledge support from the German Research Foundation (DFG) research training group GRK 2158. R.K. further wants to thank the Federal Ministry of Education and Research (BMBF; 16GW0109). H.S.A. ex-

DOI: 10.1021/acsinfecdis.7b00055
ACS Infect. Dis. 2018, 4, 123−134

presses his gratitude to the DAAD (German Academic Exchange Service) for a doctoral scholarship. R.K. thanks William R. Jacobs Jr. (Albert Einstein College of Medicine, Bronx, USA) for provision of XDR-TB strains.

REFERENCES

(1) Raviglione, M. (2006) XDR-TB: entering the post-antibiotic era? *Int. J. Tuberc. Lung Dis. 10*, 1185−1187.
(2) Shenoi, S., and Friedland, G. (2009) Extensively drug-resistant tuberculosis: a new face to an old pathogen. *Annu. Rev. Med. 60*, 307−320.
(3) Ginsberg, A. M. (2010) Tuberculosis drug development: progress, challenges, and the road ahead. *Tuberculosis 90*, 162−167.
(4) Ginsberg, A. M. (2010) Drugs in development for tuberculosis. *Drugs 70*, 2201−2214.
(5) Wong, E. B., Cohen, K. A., and Bishai, W. R. (2013) Rising to the challenge: new therapies for tuberculosis. *Trends Microbiol. 21*, 493.
(6) Cohen, J. (2013) Infectious disease. Approval of novel TB drug celebrated−with restraint. *Science 339*, 130.
(7) Ryan, N. J., and Lo, J. H. (2014) Delamanid: first global approval. *Drugs 74*, 1041−1045.
(8) Andries, K., Verhasselt, P., Guillemont, J., Gohlmann, H. W., Neefs, J. M., Winkler, H., Van Gestel, J., Timmerman, P., Zhu, M., Lee, E., Williams, P., de Chaffoy, D., Huitric, E., Hoffner, S., Cambau, E., Truffot-Pernot, C., Lounis, N., and Jarlier, V. (2005) A diarylquinoline drug active on the ATP synthase of Mycobacterium tuberculosis. *Science 307*, 223−227.
(9) Newman, D. J., and Cragg, G. M. (2012) Natural products as sources of new drugs over the 30 years from 1981 to 2010. *J. Nat. Prod. 75*, 311−335.
(10) Copp, B. R., and Pearce, A. N. (2007) Natural product growth inhibitors of Mycobacterium tuberculosis. *Nat. Prod. Rep. 24*, 278−297.
(11) Ashforth, E. J., Fu, C., Liu, X., Dai, H., Song, F., Guo, H., and Zhang, L. (2010) Bioprospecting for antituberculosis leads from microbial metabolites. *Nat. Prod. Rep. 27*, 1709−1719.
(12) Garcia, A., Bocanegra-Garcia, V., Palma-Nicolas, J. P., and Rivera, G. (2012) Recent advances in antitubercular natural products. *Eur. J. Med. Chem. 49*, 1−23.
(13) Daletos, G., Kalscheuer, R., Koliwer-Brandl, H., Hartmann, R., de Voogd, N. J., Wray, V., Lin, W., and Proksch, P. (2015) Callyaerins from the Marine Sponge Callyspongia aerizusa: Cyclic Peptides with Antitubercular Activity. *J. Nat. Prod. 78*, 1910−1925.
(14) Marchelli, R., and Vining, L. C. (1975) Terphenyllin, a novel p-terphenyl metabolite from aspergillus candidus. *J. Antibiot. 28*, 328−331.
(15) Marchelli, R., and Vining, L. C. (1973) The biosynthetic origin of chlorflavonin, a flavonoid antibiotic from Aspergillus candidus. *Can. J. Biochem. 51*, 1624−1629.
(16) Bird, A. E., and Marshall, A. C. (1969) Structure of chlorflavonin. *J. Chem. Soc. C 18*, 2418−2420.
(17) Watanabe, S., Hirai, H., Kato, Y., Nishida, H., Saito, T., Yoshikawa, N., Parkinson, T., and Kojima, Y. (2001) CJ-19,784, a new antifungal agent from a fungus, Acanthostigmella sp. *J. Antibiot. 54*, 1031−1035.
(18) Hoagland, D. T., Liu, J., Lee, R. B., and Lee, R. E. (2016) New agents for the treatment of drug-resistant Mycobacterium tuberculosis. *Adv. Drug Delivery Rev. 102*, 55−72.
(19) Richards, M., Bird, A. E., and Munden, J. E. (1969) Chlorflavonin, a New Antifungal Antibiotic. *J. Antibiot. 22*, 388−389.
(20) Liu, Y., Li, Y., and Wang, X. (2016) Acetohydroxyacid synthases: evolution, structure, and function. *Appl. Microbiol. Biotechnol. 100*, 8633−8649.
(21) Webb, M. E., Smith, A. G., and Abell, C. (2004) Biosynthesis of pantothenate. *Nat. Prod. Rep. 21*, 695−721.
(22) McCourt, J. A., Pang, S. S., Guddat, L. W., and Duggleby, R. G. (2005) Elucidating the specificity of binding of sulfonylurea herbicides to acetohydroxyacid synthase. *Biochemistry 44*, 2330−2338.
(23) Choi, K. J., Yu, Y. G., Hahn, H. G., Choi, J. D., and Yoon, M. Y. (2005) Characterization of acetohydroxyacid synthase from Mycobacterium tuberculosis and the identification of its new inhibitor from the screening of a chemical library. *FEBS Lett. 579*, 4903−4910.
(24) Hondalus, M. K., Bardarov, S., Russell, R., Chan, J., Jacobs, W. R., Jr., and Bloom, B. R. (2000) Attenuation of and protection induced by a leucine auxotroph of Mycobacterium tuberculosis. *Infect. Immun. 68*, 2888−2898.
(25) Sambandamurthy, V. K., Wang, X., Chen, B., Russell, R. G., Derrick, S., Collins, F. M., Morris, S. L., and Jacobs, W. R., Jr (2002) A pantothenate auxotroph of Mycobacterium tuberculosis is highly attenuated and protects mice against tuberculosis. *Nat. Med. 8*, 1171−1174.
(26) Sampson, S. L., Dascher, C. C., Sambandamurthy, V. K., Russell, R. G., Jacobs, W. R., Jr., Bloom, B. R., and Hondalus, M. K. (2004) Protection elicited by a double leucine and pantothenate auxotroph of Mycobacterium tuberculosis in guinea pigs. *Infect. Immun. 72*, 3031−3037.
(27) Sampson, S. L., Mansfield, K. G., Carville, A., Magee, D. M., Quitugua, T., Howerth, E. W., Bloom, B. R., and Hondalus, M. K. (2011) Extended safety and efficacy studies of a live attenuated double leucine and pantothenate auxotroph of Mycobacterium tuberculosis as a vaccine candidate. *Vaccine 29*, 4839−4847.
(28) Awasthy, D., Gaonkar, S., Shandil, R. K., Yadav, R., Bharath, S., Marcel, N., Subbulakshmi, V., and Sharma, U. (2009) Inactivation of the ilvB1 gene in Mycobacterium tuberculosis leads to branched-chain amino acid auxotrophy and attenuation of virulence in mice. *Microbiology 155*, 2978−2987.
(29) Singh, V., Chandra, D., Srivastava, B. S., and Srivastava, R. (2011) Biochemical and transcription analysis of acetohydroxyacid synthase isoforms in Mycobacterium tuberculosis identifies these enzymes as potential targets for drug development. *Microbiology 157*, 29−37.
(30) Chaleff, R. S., and Mauvais, C. J. (1984) Acetolactate synthase is the site of action of two sulfonylurea herbicides in higher plants. *Science 224*, 1443−1445.
(31) Shaner, D. L., Anderson, P. C., and Stidham, M. A. (1984) Imidazolinones - Potent Inhibitors of Acetohydroxyacid Synthase. *Plant Physiol. 76*, 545−546.
(32) Dong, M., Wang, D., Jiang, Y., Zhao, L., Yang, C., and Wu, C. (2011) In vitro efficacy of acetohydroxyacid synthase inhibitors against clinical strains of Mycobacterium tuberculosis isolated from a hospital in Beijing, China. *Saudi Med. J. 32*, 1122−1126.
(33) Gokhale, K., and Tilak, B. (2015) Mechanisms of Bacterial Acetohydroxyacid Synthase (AHAS) and Specific Inhibitors of Mycobacterium tuberculosis AHAS as Potential Drug Candidates Against Tuberculosis. *Curr. Drug Targets 16*, 689−699.
(34) Liu, Y., Bao, P., Wang, D., Li, Z., Li, Y., Tang, L., Zhou, Y., and Zhao, W. (2014) Evaluation of the in vivo efficacy of novel monosubstituted sulfonylureas against H37Rv and extensively drug-resistant tuberculosis. *Jpn. J. Infect. Dis. 67*, 485−487.
(35) Sohn, H., Lee, K. S., Ko, Y. K., Ryu, J. W., Woo, J. C., Koo, D. W., Shin, S. J., Ahn, S. J., Shin, A. R., Song, C. H., Jo, E. K., Park, J. K., and Kim, H. J. (2008) In vitro and ex vivo activity of new derivatives of acetohydroxyacid synthase inhibitors against Mycobacterium tuberculosis and non-tuberculous mycobacteria. *Int. J. Antimicrob. Agents 31*, 567−571.
(36) Wang, D., Pan, L., Cao, G., Lei, H., Meng, X., He, J., Dong, M., Li, Z., and Liu, Z. (2012) Evaluation of the in vitro and intracellular efficacy of new monosubstituted sulfonylureas against extensively drug-resistant tuberculosis. *Int. J. Antimicrob. Agents 40*, 463−466.
(37) Wang, D., Zhu, X. L., Cui, C. J., Dong, M., Jiang, H. L., Li, Z. M., Liu, Z., Zhu, W. L., and Wang, J. G. (2013) Discovery of Novel Acetohydroxyacid Synthase Inhibitors as Active Agents against Mycobacterium tuberculosis by Virtual Screening and Bioassay. *J. Chem. Inf. Model. 53*, 343−353.
(38) Grandoni, J. A., Marta, P. T., and Schloss, J. V. (1998) Inhibitors of branched-chain amino acid biosynthesis as potential antituberculosis agents. *J. Antimicrob. Chemother. 42*, 475−482.

DOI: 10.1021/acsinfecdis.7b00055
ACS Infect. Dis. 2018, 4, 123−134

(39) Kjer, J., Debbab, A., Aly, A. H., and Proksch, P. (2010) Methods for isolation of marine-derived endophytic fungi and their bioactive secondary products. *Nat. Protoc. 5*, 479−490.
(40) Ioerger, T. R., Feng, Y. C., Ganesula, K., Chen, X. H., Dobos, K. M., Fortune, S., Jacobs, W. R., Mizrahi, V., Parish, T., Rubin, E., Sassetti, C., and Sacchettini, J. C. (2010) Variation among Genome Sequences of H37Rv Strains of Mycobacterium tuberculosis from Multiple Laboratories. *J. Bacteriol. 192*, 3645−3653.
(41) CLSI. (2012) Methods for Dilution Antimicrobial Susceptibility Tests for Bacteria That Grow Aerobically, in *Approved Standard*, Ninth ed., Clinical and Laboratory Standards Institute, Wayne, PA.
(42) Kerry, D. W., Hamilton-Miller, J. M., and Brumfitt, W. (1975) Trimethoprim and rifampicin: in vitro activities separately and in combination. *J. Antimicrob. Chemother. 1*, 417−427.
(43) Martin, C. J., Booty, M. G., Rosebrock, T. R., Nunes-Alves, C., Desjardins, D. M., Keren, I., Fortune, S. M., Remold, H. G., and Behar, S. M. (2012) Efferocytosis Is an Innate Antibacterial Mechanism. *Cell Host Microbe 12*, 289−300.
(44) Larsen, M. H., Biermann, K., Tandberg, S., Hsu, T., and Jacobs, W. R., Jr. (2007) Genetic Manipulation of *Mycobacterium tuberculosis*, in *Current Protocols in Microbiology*, pp 10A.12.12−10A.12.13, John Wiley & Sons Inc, New York.
(45) Ioerger, T. R., Feng, Y., Ganesula, K., Chen, X., Dobos, K. M., Fortune, S., Jacobs, W. R., Jr., Mizrahi, V., Parish, T., Rubin, E., Sassetti, C., and Sacchettini, J. C. (2010) Variation among genome sequences of H37Rv strains of Mycobacterium tuberculosis from multiple laboratories. *J. Bacteriol. 192*, 3645−3653.
(46) Gohlke, H., Hergert, U., Meyer, T., Mulnaes, D., Grieshaber, M. K., Smits, S. H., and Schmitt, L. (2013) Binding region of alanopine dehydrogenase predicted by unbiased molecular dynamics simulations of ligand diffusion. *J. Chem. Inf. Model. 53*, 2493−2498.
(47) Widderich, N., Pittelkow, M., Hoppner, A., Mulnaes, D., Buckel, W., Gohlke, H., Smits, S. H., and Bremer, E. (2014) Molecular dynamics simulations and structure-guided mutagenesis provide insight into the architecture of the catalytic core of the ectoine hydroxylase. *J. Mol. Biol. 426*, 586−600.
(48) Jacobson, M. P., Friesner, R. A., Xiang, Z., and Honig, B. (2002) On the role of the crystal environment in determining protein side-chain conformations. *J. Mol. Biol. 320*, 597−608.
(49) Jorgensen, W. L., and Tirado-Rives, J. (1988) The OPLS [optimized potentials for liquid simulations] potential functions for proteins, energy minimizations for crystals of cyclic peptides and crambin,. *J. Am. Chem. Soc. 110*, 1657−1666.
(50) Schrödinger. (2014) *Glide* v. 6.2, Schrödinger, LLC, New York, NY.
(51) Friesner, R. A., Banks, J. L., Murphy, R. B., Halgren, T. A., Klicic, J. J., Mainz, D. T., Repasky, M. P., Knoll, E. H., Shelley, M., Perry, J. K., Shaw, D. E., Francis, P., and Shenkin, P. S. (2004) Glide: a new approach for rapid, accurate docking and scoring. 1. Method and assessment of docking accuracy. *J. Med. Chem. 47*, 1739−1749.
(52) Österberg, F., Morris, G. M., Sanner, M. F., Olson, A. J., and Goodsell, D. S. (2002) Automated docking to multiple target structures: incorporation of protein mobility and structural water heterogeneity in AutoDock. *Proteins: Struct., Funct., Genet. 46*, 34−40.
(53) Morris, G. M., Goodsell, D. S., Halliday, R. S., Huey, R., Hart, W. E., Belew, R. K., and Olson, A. J. (1998) Automated docking using a Lamarckian genetic algorithm and an empirical binding free energy function. *J. Comput. Chem. 19*, 1639−1662.
(54) Gohlke, H., Hendlich, M., and Klebe, G. (2000) Knowledge-based scoring function to predict protein-ligand interactions. *J. Mol. Biol. 295*, 337−356.
(55) Radestock, S., Bohm, M., and Gohlke, H. (2005) Improving binding mode predictions by docking into protein-specifically adapted potential fields. *J. Med. Chem. 48*, 5466−5479.
(56) Sotriffer, C. A., Gohlke, H., and Klebe, G. (2002) Docking into knowledge-based potential fields: A comparative evaluation of DrugScore. *J. Med. Chem. 45*, 1967−1970.

DOI: 10.1021/acsinfecdis.7b00055
ACS Infect. Dis. 2018, 4, 123−134